Structural Investigations with the Dipolar Demagnetizing Field in Solution NMR

R. Bowtell and P. Robyr

Magnetic Resonance Centre, University of Nottingham, Nottingham NG7 2RD, England

(Received 14 February 1996)

We have established a simple Fourier-space relationship between the structure of heterogeneous samples and the amplitude of multiple spin echoes which arise in solution NMR as a result of the dipolar nuclear demagnetizing field. We have also developed a pulse sequence optimized for structure measurements in two component systems. The new formalism predicts the behavior of multiple spin echoes well and gives a very good description of experimental data obtained from simply structured samples. [S0031-9007(96)00386-9]

PACS numbers: 76.60.Lz, 61.20.–p, 76.60.Pc

The effect of the dipolar nuclear demagnetizing field is generally neglected in nuclear magnetic resonance (NMR) of liquids, since it is many orders of magnitude weaker than any applied magnetic fields. In experiments which lead to the production of spatially modulated nuclear magnetization, the dipolar demagnetizing field can, however, cause a significant perturbation of the evolution of magnetization. In particular, in a conventional spin echo experiment [1], where a sequence of two radio-frequency (rf) pulses applied at times 0 and τ_e normally produces a single echo of the NMR signal at time $2\tau_e$, the dipolar demagnetizing field leads to the production of multiple spin echoes (MSE) occurring at multiples of τ_e larger than 2 [2–7]. Signals equivalent to MSE also appear in two-dimensional NMR experiments utilizing pulsed magnetic field gradients. These signals give rise to unexpected cross peaks in the resulting spectra [8–10].

Recently, it has been proposed that through manipulation of the demagnetizing field MSE may be used to extract structural information [10]. This is possible because in the presence of spatially modulated magnetization the demagnetizing field, experienced by a particular nuclear spin, results predominantly from the local magnetization found at a distance less than the spatial period of modulation [9]. By adjusting this period, structure may therefore be probed at varying length scales. All the magnetization contributes to the NMR signal in such experiments, irrespective of the period of spatial modulation. Consequently, there is no reduction in sensitivity on moving to finer resolution, and the achievable resolution is set by the mobility of the spin bearing molecules rather than by direct signal to noise ratio considerations as in conventional magnetic resonance imaging [10]. Mobility is important since the MSE result from dipolar interactions which are not averaged to zero on the experimental time scale. In liquids, such as water, diffusion thus sets a lower limit to the resolution of the order of 10 μm.

In this Letter we demonstrate how a simple and direct relation between the structure under investigation and the amplitude of the MSE may be developed. We also introduce a new experiment to create MSE between two components with different resonance frequencies. Theoretical predictions are compared with experimental results obtained by application of this sequence to a set of simple structures.

MSE are generated by the dipolar demagnetizing field, $\mathbf{B}^{\mathrm{dip}}(\mathbf{r})$, when spatially modulated transverse magnetization evolves in the presence of longitudinal magnetization which is modulated with the same spatial frequency. Such spatial modulation can be produced by the application of suitable combinations of rf pulses and pulsed magnetic field gradients [2–10]. For times of evolution t, such that $\gamma B^{\mathrm{dip}} t \ll 1$, where γ is the magnetogyric ratio, the demagnetizing field generates a small perturbation of the local magnetization $\mathbf{M}$ to give

$$\delta\mathbf{M}(\mathbf{r},t) = \mathbf{M}(\mathbf{r},t) - \mathbf{M}(\mathbf{r},0) \approx \gamma\mathbf{M}(\mathbf{r},0) \times \mathbf{B}^{\mathrm{dip}}(\mathbf{r})t\,. \tag{1}$$

MSE are produced by the resulting transverse magnetization components, δM_x and δM_y.

When the polarizing field $\mathbf{B}_0$ and the equilibrium magnetization vector $\mathbf{M}_0$ obey the condition $B_0 \gg \mu_0 M_0$, only the secular part of the demagnetizing field is relevant [2]. In this case, $\mathbf{B}^{\mathrm{dip}}$ is given by

$$\mathbf{B}^{\mathrm{dip}}(\mathbf{r}) = -\frac{\mu_0}{4\pi}\int_{-\infty}^{+\infty} d^3\mathbf{r}'\,\frac{3\cos^2\theta_{rr'} - 1}{2|r - r'|^3} \times [\mathbf{M}(\mathbf{r}') - 3M_z(\mathbf{r}')\hat{\mathbf{z}}], \tag{2}$$

where $\hat{\mathbf{z}}$ is a unit vector in the direction of the polarizing field and $\theta_{rr'}$ is the angle between $\mathbf{r} - \mathbf{r}'$ and $\hat{\mathbf{z}}$. This relation can be considerably simplified by Fourier transformation [2], which yields

$$\mathbf{B}^{\mathrm{dip}}(\mathbf{k}) = -\frac{1}{3}\mu_0\,\frac{3(\hat{\mathbf{k}}\cdot\hat{\mathbf{z}})^2 - 1}{2}[\mathbf{M}(\mathbf{k}) - 3M_z(\mathbf{k})\hat{\mathbf{z}}], \tag{3}$$

with

$$\mathbf{B}^{\mathrm{dip}}(\mathbf{k}) = \int_{-\infty}^{+\infty} d^3r\,\exp(-i\mathbf{k}\cdot\mathbf{r})\mathbf{B}^{\mathrm{dip}}(\mathbf{r}) \tag{4}$$

and

$$\mathbf{M}(\mathbf{k}) = \int_{-\infty}^{+\infty} d^3r \exp(-i\mathbf{k}\cdot\mathbf{r})\mathbf{M}(\mathbf{r}), \qquad (5)$$

while $\hat{\mathbf{k}} = \mathbf{k}/k$. Using Eqs. (1) and (3), we find that at time t the total transverse magnetization of the spin species j generated by the demagnetizing field, $\mathbf{B}^{\mathrm{dip}}$, is

$$\begin{aligned}\delta M_j^{\Sigma}(t) &= \int_{-\infty}^{+\infty} d^3r\,(\delta M_{xj} + i\delta M_{yj}) \\ &= -\frac{i\mu_0\gamma_j t}{8\pi^3}\int_{-\infty}^{+\infty} d^3k \\ &\quad\times M_j^{+}(\mathbf{k})\sum_{l=1}^{N}\alpha_{jl}M_{zl}^{*}(\mathbf{k})\Lambda(\mathbf{k}), \qquad (6)\end{aligned}$$

where $M_j^{+}(\mathbf{k})$ is the Fourier transform of $M_{xj}(\mathbf{r},0) + iM_{yj}(\mathbf{r},0)$ and $\Lambda(\mathbf{k}) = [3(\hat{\mathbf{k}}\cdot\hat{\mathbf{z}})^2 - 1]/2$. The sum in the integral runs over the N different spins species, and α_{jl} is equal to $2/3$ when the difference in resonance frequencies $|\Omega_j - \Omega_l| \gg \mu_0\gamma_j M_{0l}$. When $\Omega_j - \Omega_l = 0$, $\alpha_{jl} = 1$. This difference arises because in the former case only the z component of $\mathbf{B}^{\mathrm{dip}}$ produced by one spin species generates a coherent effect on the evolution of the transverse magnetization of the other spins.

Inspection of Eq. (6) indicates that the magnitude of the MSE depends on the overlap of the $M_{zl}(\mathbf{k})$ and $M_j^{+}(\mathbf{k})$, and on the variation of $\Lambda(\mathbf{k})$ within the region of overlap. Each of the magnetization components will show a variation with $\mathbf{k}$, dependent upon the spatial modulation imposed by applied field gradients, and upon the distribution of magnetization at equilibrium, $\sum_{l=1}^{N} M_{0l}(\mathbf{r})$. The latter reflects the structure of the sample. In experiments focusing on MSE, pulsed magnetic field gradients are generally applied so that the longitudinal and transverse magnetization of each spin species can be written in the form $M_l^{+}(\mathbf{r}) = M_{0l}(\mathbf{r})\sum_{n=-\infty}^{\infty} a_{n,l}e^{in\mathbf{k}_m\cdot\mathbf{r}}$ and $M_{zl}(\mathbf{r}) = M_{0l}(\mathbf{r})\sum_{n=-\infty}^{\infty} b_{n,l}e^{in\mathbf{k}_m\cdot\mathbf{r}}$. This implies that $M_l^{+}(\mathbf{k}) = \sum_{n=-\infty}^{\infty} a_{n,l}M_{0l}(\mathbf{k} - n\mathbf{k}_m)$ and $M_{zl}(\mathbf{k}) = \sum_{n=-\infty}^{\infty} b_{n,l}M_{0l}(\mathbf{k} - n\mathbf{k}_m)$. Here $\mathbf{k}_m$ describes a fundamental frequency of spatial modulation, which would be produced, for example, by evolution of the transverse magnetization of species l, under a linear gradient of strength G which is applied in the direction $\hat{\mathbf{s}}$ for a time, τ_G, so that $\mathbf{k}_m = \gamma_l G\tau_G\hat{\mathbf{s}}$. The values of the coefficients $a_{n,l}$ and $b_{n,l}$ depend upon the particular sequence of rf and gradient pulses employed. Large MSE can occur when the product of $a_{n,j}$ and $b_{-n,l}$ is nonzero for one or more values of n, since this will yield a significant overlap of $M_{zl}^{*}(\mathbf{k})$ and $M_j^{+}(\mathbf{k})$ in the integral of Eq. (6).

The pulse sequence, shown in Fig. 1, has been designed for structure measurements in samples containing nuclei with two distinct resonant frequencies, Ω_1 and Ω_2. In the period that extends up to the third selective pulse, the magnetization of the first component is sinusoidally modulated along the direction $\hat{\mathbf{s}}$. The gradient pulse after the third selective pulse imposes a helical modulation of the same spatial frequency on the transverse magnetization of the second component. After the application of this sequence, the only nonzero terms in the Fourier expansions are $a_{-1,2} = 1$ and $b_{-1,1} = b_{1,1} = 1/2$, so that the amplitude of the MSE at time t is

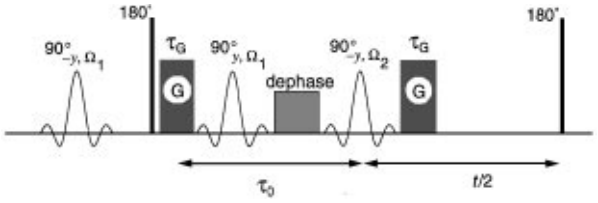

FIG. 1. Pulse sequence used to measure a multiple spin echo at a time t after the last 90° selective pulse. The first 90° pulse selectively rotates the magnetization of the component resonating at frequency Ω_1 into the transverse plane. This magnetization is spatially modulated by the application of a linear magnetic field gradient pulse of strength G and duration τ_G along a direction $\hat{\mathbf{s}}$. The second selective pulse at frequency Ω_1 tips a part of the modulated magnetization back along the $\hat{\mathbf{z}}$ direction. The remaining transverse magnetization is strongly dephased by gradient pulses. The second gradient pulse applied in the $\hat{\mathbf{s}}$ direction modulates the transverse magnetization generated by the selective pulse at frequency Ω_2. The two hard 180° pulses refocus the effects of static magnetic field inhomogeneity not generated by the demagnetizing field. They do not perturb the evolution of the MSE.

$$\begin{aligned}\delta M_2^{\Sigma}(t) &= -\frac{i\mu_0\gamma_2 t}{24\pi^3}\int_{-\infty}^{+\infty} d^3k \\ &\quad\times [M_{01}^{*}(\mathbf{k} - \mathbf{k}_m) + M_{01}^{*}(\mathbf{k} + \mathbf{k}_m)] \\ &\quad\times M_{02}(\mathbf{k} + \mathbf{k}_m)\Lambda(\mathbf{k}). \qquad (7)\end{aligned}$$

We have assumed the difference in resonance frequency is large enough to make $\alpha_{21} = 2/3$. This equation yields some insight into the relation between structure and MSE amplitude, for varying degrees of modulation. The MSE amplitude tends to zero as $\mathbf{k}_m$ is decreased to zero. For larger values of $\mathbf{k}_m$, such that neither $M_{01}(\mathbf{k})$ nor $M_{02}(\mathbf{k})$ have significant contributions for $\mathbf{k}$ values where $\mathbf{k}\cdot\hat{\mathbf{s}} \geq k_m$ (condition 1), the MSE is exclusively generated by the product of $M_{01}^{*}(\mathbf{k} + \mathbf{k}_m)$ and $M_{02}(\mathbf{k} + \mathbf{k}_m)$ in Eq. (7), which may now be written as

$$\delta M_2^{\Sigma}(t) = -\frac{i\mu_0\gamma_2 t}{24\pi^3}\int_{-\infty}^{+\infty} d^3k\, M_{01}^{*}(\mathbf{k})M_{02}(\mathbf{k})\Lambda(\mathbf{k} - \mathbf{k}_m). \qquad (8)$$

Even when this condition is not obeyed, the contribution from the term $M_{01}(\mathbf{k} - \mathbf{k}_m)$ can be eliminated by phase cycling. As $\mathbf{k}_m$ is increased further to a level where $\Lambda(\mathbf{k} - \mathbf{k}_m) \approx \Lambda(-\mathbf{k}_m)$, for all values of $\mathbf{k}$ where $M_{01}(\mathbf{k})$ and $M_{02}(\mathbf{k})$ are nonzero (condition 2), Eq. (8) reduces to an integral of the form

$$\delta M_2^{\Sigma}(t) = -\frac{i\mu_0\gamma_2 t}{3}\Lambda(\mathbf{k}_m)\int_{-\infty}^{\infty} d^3r\, M_{01}(\mathbf{r})M_{02}(\mathbf{r}), \qquad (9)$$

so that δM_2^{Σ} depends only on the direction of modulation and the overlap of the magnetization distributions. In this situation, the dipolar demagnetizing field is a simple, local function of the magnetization [2]. Clearly, Eq. (9) implies that for large $\mathbf{k}_m$ the MSE amplitude will be zero when $M_{01}(\mathbf{r})$ and $M_{02}(\mathbf{r})$ do not overlap. For values of $\mathbf{k}_m$ between the two limits described above, δM_2^{Σ} depends on the variation of $\Lambda(\mathbf{k} - \mathbf{k}_m)$, in the region where the product of $M_{01}^*(\mathbf{k})$ and $M_{02}(\mathbf{k})$ takes significant values.

All the above observations are consistent with the previously described behavior of the MSE seen in the correlated spectroscopy revamped by asymmetric z-gradient echo detection (CRAZED) experiments applied to simply structured samples [10]. In the CRAZED experiment, a gradient pulse of duration τ_G is sandwiched between two $(90°)_y$ rf pulses. The second rf pulse is followed by a second gradient pulse of the same strength, but of duration $2\tau_G$. This sequence generates longitudinal and transverse magnetization such that the only nonzero coefficients in the Fourier expansion are $a_{-1,l} = -a_{-3,l} = b_{-1,l} = b_{1,l} = -1/2$ for all N components. In the case of a two component system, the amplitude of the total transverse magnetization of the second spin species generated by the demagnetizing field at time t after the second rf pulse is given by

$$\delta M_2^{\Sigma}(t) = -\frac{i\mu_0\gamma_2 t}{32\pi^3}\int_{-\infty}^{+\infty} d^3k \left\{\frac{2}{3}[M_{01}^*(\mathbf{k} - \mathbf{k}_m) + M_{01}^*(\mathbf{k} + \mathbf{k}_m)] + [M_{02}^*(\mathbf{k} - \mathbf{k}_m) + M_{02}^*(\mathbf{k} + \mathbf{k}_m)]\right\}[M_{02}(\mathbf{k} + \mathbf{k}_m) - M_{02}(\mathbf{k} + 3\mathbf{k}_m)]\Lambda(\mathbf{k}). \quad (10)$$

The behavior of the MSE originating from the demagnetizing field of both components can be discussed along the same lines as above. When condition 1 is fulfilled, the transverse magnetization, δM_2^{Σ}, created in Eq. (10) by the action of the demagnetizing field of the first component is half as much as in the experiment of Fig. 1, described by Eq. (8).

In interpreting structure measurements, it is useful to normalize the measured MSE amplitude, S_{MSE}. This can be accomplished by measuring the ratio of S_{MSE} and the signal, S_{DE}, generated in a normal spin echo experiment carried out, for example, on the second component. If $M_{02}(\mathbf{r})$ takes only two values M_{02} and zero, the ratio of signals for the experiment of Fig. 1 is

$$\frac{S_{\mathrm{MSE}}(t)}{S_{\mathrm{DE}}} = \frac{\gamma_2\mu_0 t}{24\pi^3 M_{02} V_2}\int_{-\infty}^{+\infty} d^3k \times M_{01}^*(\mathbf{k})M_{02}(\mathbf{k})\Lambda(\mathbf{k} - \mathbf{k}_m), \quad (11)$$

where V_2 is the volume occupied by the second component. Measuring this ratio also has the advantage of partially compensating for pulse imperfections and possible T_2 relaxation effects.

An important consideration in making structure measurements via MSE is the role of diffusion. In the analysis above, the averaging of the dipolar interactions at distances up to 10 μm, as a result of diffusion on the NMR time scale, has been exploited as the reason for considering the media continuous. If the dimensions of the structure under investigation are well above this size and mobility is unrestricted along the modulation direction, it can be shown, using the formalism of Refs. [3] and [4], that the diffusion attenuation of MSE in the experiment of Fig. 1 is given by

$$S_{\mathrm{MSE}}^D(t) = S_{\mathrm{MSE}}(t)\frac{e^{-k_m^2 D_1\tau_0}(1 - e^{-k_m^2(D_1+D_2)t})}{k_m^2(D_1 + D_2)t}. \quad (12)$$

Here the diffusion coefficients of the first and second components are D_1 and D_2, respectively. When the characteristic dimensions of the structure are commensurate with the range over which diffusion nulls dipolar interactions, accounting for mobility is more complicated and will be the subject of further investigations.

Generation of MSE by the dipolar demagnetizing field has often been discussed in conjunction with radiation damping [8,11,12]. Although the two effects differ fundamentally, they are both potentially relevant in highly polarized samples. The effect of radiation damping on the experiment of Fig. 1 is limited, since the dephasing induced by the gradient pulses ensures that the total transverse magnetization vector is small during the long period when the MSE is forming.

In order to compare our theoretical model with experimental data, we measured MSE with the experiment shown in Fig. 1 in five simple structures. These consisted of two coaxial glass tubes, the outer one filled with water (component 1) and the inner one with acetone (component 2). The internal radius of the glass wall of the inner tube, a, its external radius, b, and the internal radius of the outer tube, c, are listed in Table I for all five structures. All the measurements were recorded on a home built 11.7 T NMR microscope [13], equipped with actively screened gradient coils. Figure 2 shows the measured and calculated variations of the ratio of the multiple spin echo and direct echo amplitudes at $t = 140$ ms as a function of k_m for the five samples of Table I. The magnetization was modulated along $\hat{\mathbf{z}}$, with $\tau_G = 1$ ms and $\tau_0 = 17$ ms.

TABLE I. Inner and outer radius, a and b, of the small tubes and inner radius, c, of the large tubes used to build the five structured samples.

Sample	a (mm)	b (mm)	c (mm)
1	0.52	0.70	2.15
2	0.49	0.65	2.15
3	0.35	0.49	2.15
4	0.32	0.44	2.15
5	0.32	0.44	0.56

The sizes of the structures are all such that Eq. (12) can be used. The 3D Fourier transform, in cylindrical coordinates, of a uniform magnetization distribution confined to a tube aligned with $\hat{\mathbf{z}}$, and of half length d and radius a, is

$$M(k_z, k_\rho, \theta) = 4\pi M_0 \frac{a \sin(k_z d) J_1(k_\rho a)}{k_z k_\rho}, \qquad (13)$$

where J_1 is the Bessel function of the first kind and of order 1. Substituting this expression into Eq. (11) with a modulation direction $\hat{\mathbf{s}} = \hat{\mathbf{z}}$, taking the limit $d \to \infty$, and using Eq. (12) yields

$$\frac{S^D_{\mathrm{MSE}}}{S_{\mathrm{DE}}} = \frac{\mu_0 \gamma_2 M_{01} e^{-k_m^2 D_1 \tau_0}(1 - e^{-k_m^2 (D_1 + D_2) t})}{3 k_m^2 (D_1 + D_2) a} \times \int_0^\infty \frac{dk_\rho}{k_\rho} \left(\frac{3k_m^2}{k_m^2 + k_\rho^2} - 1 \right) J_1(k_\rho a) \times [c J_1(k_\rho c) - b J_1(k_\rho b)]. \qquad (14)$$

The lines in Fig. 2 show the calculated ratio of $S^D_{\mathrm{MSE}}/S_{\mathrm{DE}}$ at $t = 140$ ms for the five structures of Table I. The attenuation due to diffusion described in Eq. (12) is weak in our experimental situation: it exceeds 10% only for $k_m > 15\ \mathrm{mm}^{-1}$. The agreement between the experimental data and the theoretical predictions is good. This is achieved in the absence of any adjustable parameters. The sequence of the curves for the four samples where the outer tube is a standard 5 mm NMR tube (samples 1–4) is well reproduced, showing that structural changes of a few tens of micrometers can be probed in simple arrangements. In all cases the ratio tends to zero as expected for large values of k_m. Systematically, however, the experimental values for the small sample (sample 5) are slightly lower than the theoretical ones, a similar trend appears for the larger samples for k_m above 10 mm^{-1}. This discrepancy may result from the effect of rf field inhomogeneity or sample misalignment.

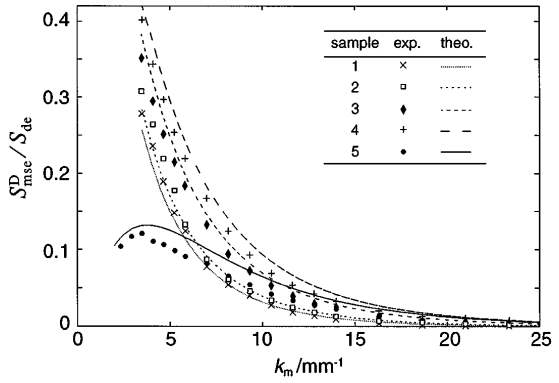

FIG. 2. Experimental and theoretical ratio $S^D_{\mathrm{MSE}}/S_{\mathrm{DE}}$ for the five samples of Table I. The MSE amplitudes were sampled at $t = 140$ ms with $\tau_0 = 17$ ms. The theoretical curves are computed from Eq. (14) using $D_1 = 2.5 \times 10^{-9}\ \mathrm{m^2\,s^{-1}}$, $D_2 = 2.1 \times 10^{-9}\ \mathrm{m^2\,s^{-1}}$, and $M_{01} = 0.0389\ \mathrm{A\,m^{-1}}$.

In conclusion, this Letter further demonstrates that structural characteristics can be probed by measuring multiple spin echoes generated by the dipolar demagnetizing field, and it establishes a simple relation between the MSE amplitude and the structure under investigation. The formalism introduced here can easily be extended to more complicated structures and to other measurement sequences. Work along these lines is currently in progress.

P. R. thanks the Swiss Science Foundation for a scholarship.

[1] E. Hahn, Phys. Rev. **80**, 580 (1950).
[2] G. Deville, M. Bernier, and J. M. Delrieux, Phys. Rev. B **19**, 5666 (1979).
[3] D. Einzel, G. Eska, Y. Hirayoshi, T. Kopp, and P. Wolfe, Phys. Rev. Lett. **53**, 2312 (1984).
[4] R. Bowtell, R. M. Bowley, and P. Glover, J. Magn. Reson. **88**, 643 (1990).
[5] A. S. Bedford, R. Bowtell, and R. M. Bowley, J. Magn. Reson. **93**, 516 (1991).
[6] R. Bowtell, J. Magn. Reson. **100**, 1 (1992).
[7] H. Körber, E. Dormann, and G. Eska, J. Magn. Reson. **93**, 589 (1991).
[8] Q. He, W. Richter, S. Vathyam, and W. S. Warren, J. Chem. Phys. **98**, 6779 (1993).
[9] W. S. Warren, W. Richter, A. H. Andreotti, and B. T. Farmer II, Science **262**, 2005 (1993).
[10] W. Richter, S. Lee, W. S. Warren, and Q. He, Science **267**, 654 (1995).
[11] A. Vlassenbroek, J. Jeener, and P. Broekaert, J. Chem. Phys. **103**, 5886 (1995).
[12] M. A. McCoy and W. S. Warren, J. Chem. Phys. **93**, 858 (1990).
[13] R. W. Bowtell, G. D. Brown, P. M. Glover, M. McJury, and P. Mansfield, Philos. Trans. R. Soc. London **333**, 457 (1990).